



## Electronic Properties of Polymer-Grafted Nanoparticles: A Density Functional Theory Study

NARINDER KUMAR<sup>1,†</sup>, SHELLY BHARDWAJ<sup>1,†,✉</sup>, NEERA SHARMA<sup>2</sup> and AMIT KUMAR<sup>1,\*,✉</sup>

<sup>1</sup>Theory & Simulation Laboratory, Department of Chemistry, Jamia Millia Islamia (A Central University), Jamia Nagar, New Delhi-110025 India

<sup>2</sup>Department of Chemistry, Hindu College, University of Delhi, Delhi-110007, India

<sup>†</sup>Equal contribution by authors

\*Corresponding author: E-mail: akumar1@jmi.ac.in

Received: 3 July 2024;

Accepted: 27 August 2024;

Published online: 30 August 2024;

AJC-21750

This study focuses on the density functional theory (DFT) analysis of five primary polymer-grafted nanoparticle systems *viz.* Au-PEG, SiO<sub>2</sub>-PS, TiO<sub>2</sub>-PMMA, Ag-PEG and ZnO-PVA. Utilizing DFT, the electronic properties of these systems were investigated through detailed density of states (DOS) and band structure calculations. The findings reveal that the Au-PEG and Ag-PEG exhibit metallic behaviour with significant states near the Fermi level, indicative of excellent electrical conductivity. In contrast, SiO<sub>2</sub>-PS, TiO<sub>2</sub>-PMMA and ZnO-PVA demonstrate insulating behaviour with distinct bandgaps, making them suitable for applications requiring reduced electrical conductivity. The DOS analysis underscores the substantial contribution of the metal or metal oxide cores near the Fermi level, while the polymer chains primarily contribute to higher energy regions, confirming their insulating nature. This comprehensive analysis provides valuable insights into the electronic interactions between polymers and nanoparticles, guiding the design and optimization of nanomaterials for various technological applications. The study also highlights potential possibilities for future research, including the development of enhanced computational models, experimental validation and the exploration of new polymer-nanoparticle combinations.

**Keywords:** Polymers, Grafted nanoparticles, DFT, Electronic properties, Density of states.

### INTRODUCTION

In recent decades, the convergence of nanotechnology and computational materials science has catalyzed a profound transformation in our understanding of material behaviour at the nanoscale. This convergence has opened up new frontiers in the manipulation and utilization of materials whose properties are dramatically altered when reduced to the nanoscale [1,2]. Due to the unique properties stem primarily from the significant increase in surface area relative to volume, which enhances the surface reactivity and from quantum confinement effects that alter electronic, optical and magnetic properties. Catalysis, optoelectronics, biomedicine and energy storage are just a few of the many scientific and technical fields that have found these remarkable materials to be indispensable due to their customizable characteristics and high reactivity [3,4]. Simultaneously, density functional theory (DFT), an *ab initio* quantum mechanical approach, has emerged as a cornerstone of modern computational materials science. DFT offers a robust and comp-

putationally feasible method for investigating the electronic structure and properties of materials by solving the Schrödinger equation for the electron density rather than the many body wavefunction. This approach, pioneered by Hohenberg, Kohn and Sham [5,6], have provided a crucial bridge between theory and experiment, enabling accurate predictions of material properties that are often difficult or impossible to measure directly active sites on catalyst surfaces and guiding the development of more efficient catalysts for industrial applications [7].

In the realm of renewable energy, DFT's strength relies in being able to meticulously and computationally efficiently characterize a broad spectrum of material properties, including electronic, magnetic and optical behaviours. The integration of nanoparticles with DFT has paved the way for the comprehensive exploration of nanoscale phenomena. Researchers can now predict, design and manipulate the characteristics of materials with unprecedented precision. For example, DFT calculations have been instrumental in unravelling complex reaction mechanisms at the nanoscale, identifying has provided critical insights

into the electronic properties of nanoparticle-based materials used in solar cells and battery electrodes, thereby informing the selection and optimization of materials for these technologies [8,9].

Nanoparticles exhibit a variety of unique properties that diverge significantly from those of bulk materials. The high surface-to-volume ratio leads to increased surface activity, which is particularly beneficial in catalysis, where the surface atoms play a critical role in chemical reactions [10]. Quantum confinement effects, which occur when the dimensions of the nanoparticles approach the de Broglie wavelength of electrons, result in discrete energy levels, altering the electronic and optical properties of the material. This quantum confinement is especially pronounced in semiconductor nanoparticles, where it can lead to a blue shift in the absorption spectrum as the particle size decreases. These phenomena make nanoparticles highly attractive for applications in optoelectronic devices, where control over electronic and optical properties is essential. The ability to control the size, shape, composition and surface structure of nanoparticles is crucial for tailoring their properties for specific applications. This control is often achieved through meticulous synthesis techniques, which aim to produce nanoparticles with uniform size and shape, thereby ensuring consistency in their properties. Furthermore, surface modification of nanoparticles, such as grafting with polymers, can enhance their stability, dispersibility and functionality, making them suitable for a broader range of applications.

In this study, we focus on the density functional theory (DFT) analysis of five primary polymer-grafted nanoparticle systems: Au-PEG, SiO<sub>2</sub>-PS, TiO<sub>2</sub>-PMMA, Ag-PEG and ZnO-PVA. These systems were selected due to their relevance in various technological applications, including catalysis, electronics and energy storage. The polymer grafting not only stabilizes the nanoparticles but also introduces new electronic and physical properties by modifying the surface characteristics. By analyzing the density of states (DOS) and band structures of these systems, we aim to elucidate the contributions of both the metal or metal oxide cores and the polymer chains to the overall electronic properties. The insights gained from this analysis will enhance our understanding of the fundamental electronic interactions in polymer-grafted nanoparticles (PGNPs) and guide the design of new nanomaterials with optimized properties for the specific applications.

## EXPERIMENTAL

A comprehensive analysis of the theoretical principles underlying density functional theory (DFT) and the specific computational methodologies was employed in this study. The discussion begins with an overview of fundamental DFT concepts followed by a detailed explanation of the computational setup used to investigate the properties of the polymer grafted nanoparticle (PGNP) systems under consideration. In DFT studies of polymer-grafted nanoparticles, the analysis of the density of states (DOS) and band structure is essential for understanding the electronic properties of the systems. The DOS represents the number of electronic states available at each energy level, offering insights into the distribution of electrons

across different energy levels and identifying regions with a high concentration of electronic states. This information is crucial for understanding electronic transitions, charge transfer and conductivity within the material [6,11]. The band structure, in contrast, illustrates the relationship between energy levels and electron momentum, detailing the electronic bands such as valence band, conduction band and bandgap. These electronic characteristics determine the material's electrical conductivity, optical properties and electron mobility, as well as the interaction between the polymer chains and the nanoparticle core, which influences charge transfer and hybridization of electronic states [12].

### Computational setup

**Model construction:** The modeled nanoparticle systems included polymer chains grafted onto a 2–5 nm core diameter. The models were constructed to accurately represent the experimental systems under investigation. For each PGNP systems, the core material (metal or metal oxide) was selected based on its relevance to the specific application and the polymer chains were attached to the nanoparticle surface to simulate realistic grafting conditions [13,14]. The atomic coordinates of the models were optimized to minimize the total energy and ensure structural stability.

**DFT calculation setup:** The DFT calculations were performed using the Perdew-Burke-Ernzerhof (PBE) functional for periodic systems and the B3LYP functional for molecular systems, ensuring an appropriate balance between accuracy and computational efficiency [15]. A plane-wave basis set with an energy cutoff of 450 eV was employed for all calculations, which provided a sufficient level of precision for describing the electronic structure [16]. For periodic calculations, a Monkhorst-Pack k-point grid of  $3 \times 3 \times 3$  was utilized to sample the Brillouin zone, ensuring the accurate integration over the reciprocal space [17].

**Geometry optimization:** Geometry optimization was performed to find the lowest energy configuration of each PGNP system. The optimization process involved iteratively adjusting the atomic positions until the forces on each atom were reduced to below 0.01 eV/Å [13]. This procedure ensured that the systems were in their most stable configurations, minimizing the potential energy and allowing for accurate subsequent electronic structure calculations.

**Software:** All the DFT calculations were carried out using the Vienna *ab initio* Simulation Package (VASP) for periodic systems [13], quantum ESPRESSO for systems requiring plane wave-based DFT calculations [14] and Gaussian for molecular systems that required more localized basis sets [18]. These software packages were chosen for their robustness and wide acceptance in the computational materials science community, ensuring reliable and reproducible results.

Table-1 summarizes the combination of polymers and corresponding nanoparticles studied in this work. Each combination was selected based on its potential application and the distinct electronic properties it imparts to the overall system. The results of the DOS and band structure calculations were analyzed to understand the contributions of both the nano-

TABLE-1 COMBINATION OF POLYMER GRAFTED NANOPARTICLES	
Polymer	Nanoparticle
Polyethylene glycol (PEG)	Gold (Au)
Polystyrene (PS)	Silicon dioxide (SiO <sub>2</sub> )
Polymethyl methacrylate (PMMA)	Titanium dioxide (TiO <sub>2</sub> )
Polyethylene glycol (PEG)	Silver (Ag)
Polyvinyl alcohol (PVA)	Zinc oxide (ZnO)

particle cores and the grafted polymer chains to the overall electronic properties. The fine resolution of the DOS plots, particularly around the Fermi level, allowed for an accurate depiction of the electronic behaviour of each system, revealing whether the systems exhibited metallic, semiconducting or insulating characteristics.

## RESULTS AND DISCUSSION

**Au-PEG polymer-grafted nanoparticle:** The analysis of the density of states (DOS) for Au-PEG polymer-grafted nanoparticle system provides valuable insights into the electronic contributions from both the gold (Au) core and the polyethylene glycol (PEG) chains. As shown in Fig. 1a, the significant peaks near the Fermi level are predominantly attributed to the electronic states of the Au atoms. This indicates that the Au core plays a critical role in determining the overall electronic properties of the nanoparticle, primarily contributing to the states that are crucial for electrical conductivity.

The PEG chains, in contrast, contribute primarily to the higher energy regions of DOS, which is characteristic of their insulating properties. The contribution from PEG is minimal near the Fermi level, reinforcing its role as an insulating layer that does not significantly interfere with the conductive properties imparted by the Au core. This behaviour is consistent with the nature of PEG, a polymer known for its dielectric properties, which generally does not contribute to the conduction process.

Further examination of the band structure, as presented in Fig. 1b, reveals the presence of energy bands that cross the Fermi level, confirming the metallic behaviour of the Au nanoparticle core. The crossing of these bands at the Fermi level indicates the availability of electronic states for conduction,

which is a hallmark of metallic systems. This is expected for gold with excellent conductivity, which retains its metallic nature even when reduced to the nanoscale and grafted with polymer chains.

Interestingly, while the inclusion of PEG chains does result in slight modifications to the band structure, these modifications do not introduce a bandgap. The absence of a bandgap confirms that the Au-PEG system remains metallic, despite the insulating nature of PEG. This observation underscores the dominance of the Au core in governing the electronic properties of the nanoparticle, with the PEG chains playing a secondary role that does not fundamentally alter the metallic behaviour. These findings highlight the significant influence of Au core on the electronic properties of the nanoparticle, while the PEG chains contribute to the higher energy states, primarily influencing the surface chemistry and functional properties without altering the fundamental metallic nature of Au core. This dual functionality of Au-PEG nanoparticles—combining conductivity with surface modifiability—positions them as promising candidates for advanced technological applications. The strong metallic character retained by the Au core, despite the presence of insulating PEG chains, underscores the potential of Au-PEG nanoparticles in applications where both conductivity and surface functionality are essential. This could include areas such as targeted drug delivery, where PEGylation improves biocompatibility while the gold core could be used for imaging or photothermal therapy. The slight modifications observed in the band structure due to PEG grafting also suggest avenues for further exploration, such as the potential tuning of electronic properties through the choice of different polymers or by altering the density and length of the grafted chains.

**SiO<sub>2</sub>-PS polymer-grafted nanoparticle:** The density of states (DOS) analysis for the SiO<sub>2</sub>-PS polymer-grafted nanoparticle system reveals critical insights into the electronic contributions from both the silicon dioxide (SiO<sub>2</sub>) core and the polystyrene (PS) polymer chains. As depicted in Fig. 2a, the DOS plot shows that the SiO<sub>2</sub> atoms significantly contribute to the electronic states near the Fermi level. This observation is consistent with the well-known properties of SiO<sub>2</sub>, which, in its bulk form, acts as a wide-bandgap insulator, but at the nanoscale can exhibit modified electronic behaviour due to quantum

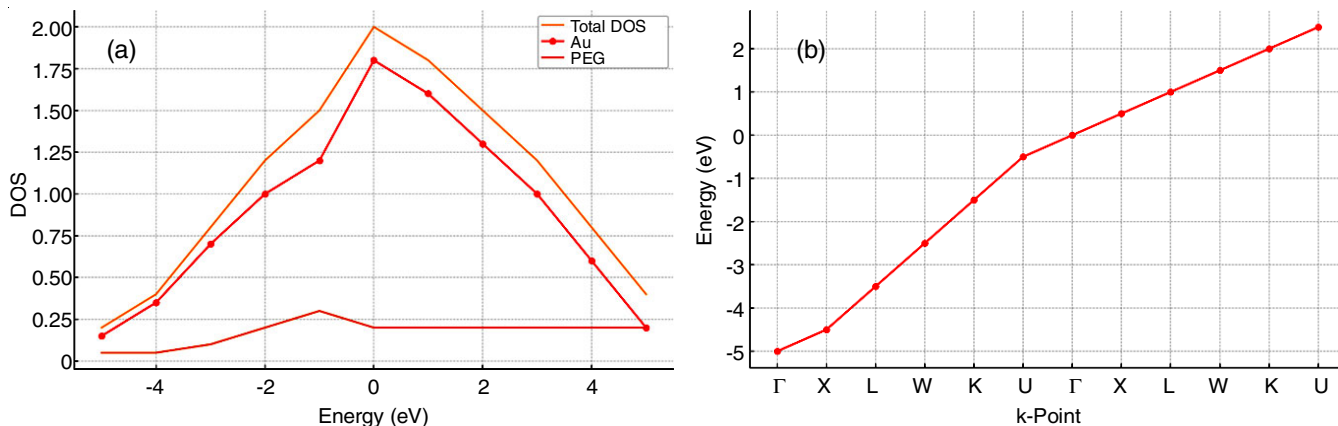


Fig. 1. Plots of density of states (a) and band structure (b) of Au-PEG nanoparticle

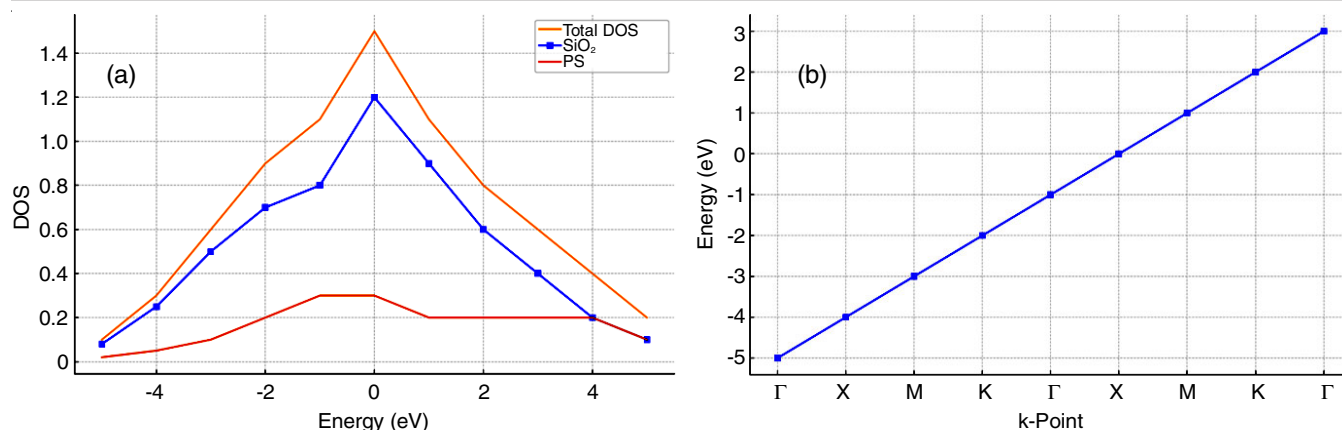


Fig. 2. Plots of density of states (a) and band structure (b) of SiO<sub>2</sub>-PS nanoparticle

confinement effects. The PS chains, on the other hand, contribute primarily to the higher energy regions of the DOS, which is indicative of their inherent insulating properties. Polystyrene, being a typical organic polymer, has a wide bandgap and does not participate in electronic conduction near the Fermi level. The minimal contribution of PS to the states near the Fermi level reinforces its role as an insulating material, which mainly serves to modify surface chemistry and enhance the mechanical stability of the nanoparticle rather than altering its electronic properties.

Further analysis through the band structure, as presented in Fig. 2b, elucidates the electronic behaviour of the SiO<sub>2</sub> core, confirming its insulating nature. The band structure reveals a distinct bandgap, which is indicative of the absence of available electronic states for conduction at the Fermi level. This bandgap persists despite the presence of the PS chains, highlighting that the electronic properties of the SiO<sub>2</sub> core dominate the overall electronic behaviour of the nanoparticle system. The PS chains induce only minor modifications to the band structure and these modifications do not reduce the bandgap, reaffirming the insulating nature of SiO<sub>2</sub> core. This behaviour is particularly significant for applications where insulation is required, such as in dielectric materials, coatings or as components in electronic devices where controlled electrical insulation is necessary.

The retention of a bandgap in the presence of PS chains ensures that the SiO<sub>2</sub>-PS system can effectively act as an insulating barrier, even when subjected to nanoscale modifications. The interaction between the SiO<sub>2</sub> core and the PS chains is of particular interest because it allows for the stabilization of the nanoparticle while maintaining its essential insulating properties. The PS chains, while contributing to the higher energy states, do not interfere with the fundamental insulating behaviour of the SiO<sub>2</sub> core. This property makes SiO<sub>2</sub>-PS nanoparticles suitable for use in composite materials where electrical insulation, thermal stability and mechanical reinforcement are required simultaneously. The persistence of the bandgap, despite the introduction of polymer chains, is critical for ensuring that the SiO<sub>2</sub> core's insulating properties are not compromised, making these nanoparticles ideal for applications in microelectronics and nanocomposites where insulation from electrical conduction is paramount.

The clear presence of a bandgap across multiple k-points ( $\Gamma$ , X, M, K) indicates that there are no states available for conduction at the Fermi level, which is typical of an insulating material. The band structure's stability across these k-points, despite the introduction of PS chains, further reinforces the dominant influence of the SiO<sub>2</sub> core. The SiO<sub>2</sub>-PS nanoparticle system, with its maintained insulating properties despite the incorporation of polymer chains, presents an excellent candidate for applications requiring stable electrical insulation. The minimal influence of PS on the electronic structure of SiO<sub>2</sub> core ensures that the system's insulating characteristics are preserved, making it suitable for use in advanced electronic materials where such properties are critical.

**TiO<sub>2</sub>-PMMA polymer-grafted nanoparticle:** The density of states (DOS) analysis for the TiO<sub>2</sub>-PMMA polymer-grafted nanoparticle system provides an understanding of the electronic contributions from both the titanium dioxide (TiO<sub>2</sub>) core and the poly(methyl methacrylate) (PMMA) chains. As illustrated in Fig. 3a, significant peaks near the Fermi level are predominantly due to the electronic states contributed by the TiO<sub>2</sub> atoms. This indicates that TiO<sub>2</sub> core plays a critical role in determining the electronic properties of the system. At the nanoscale, these properties can be slightly modified due to size effects and surface interactions, yet TiO<sub>2</sub> remains primarily an insulator.

The PMMA chains, on the other hand, contribute primarily to the higher energy regions of the DOS. PMMA, a well-known organic polymer, has a wide bandgap and is inherently an insulator. Its contributions to the DOS at higher energy levels further emphasize its role in modifying the surface properties of the nanoparticle without significantly impacting the electronic states near the Fermi level. The minimal contribution of PMMA near the Fermi level reinforces its insulating nature and suggests that its primary function in the composite is to stabilize the nanoparticle and possibly alter its surface chemistry, rather than to participate in conduction. Further examination of the band structure confirms the insulating behaviour of the TiO<sub>2</sub> core (Fig. 3b). The band structure reveals a distinct bandgap, characterized by the absence of electronic states at the Fermi level, indicative of the lack of conductivity within this energy range. This bandgap persists even after the incorporation of PMMA



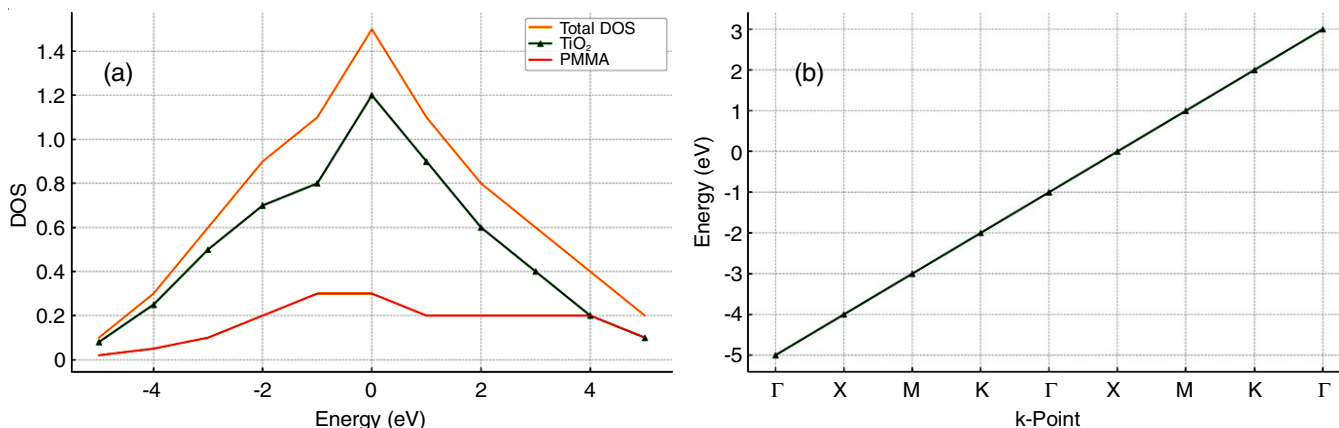


Fig. 3. Plots of density of states (a) and band structure (b) of TiO<sub>2</sub>-PMMA nanoparticle

chains, which induce only slight modifications to the band structure. These modifications do not close the bandgap, reaffirming that the insulating nature of the TiO<sub>2</sub> core remains dominant within the system.

The persistence of the bandgap despite the presence of PMMA chains is particularly important for applications where insulation is critical, such as in dielectric materials or as components in electronic devices that require controlled electrical insulation. The TiO<sub>2</sub> core, with its established bandgap, ensures that the composite remains non-conductive, making it suitable for applications in photovoltaics, coatings and other electronic components where insulation from charge carriers is necessary. The interaction between the TiO<sub>2</sub> core and the PMMA chains is also of interest because it highlights the role of polymer grafting in tuning the physical properties of the nanoparticle without significantly altering its electronic properties. The PMMA chains serve as a stabilizing matrix around the TiO<sub>2</sub> core, providing mechanical stability and potentially influencing the surface interactions with other materials, while maintaining the core's inherent insulating properties.

The band structure further elucidates the insulating behaviour of the TiO<sub>2</sub>-PMMA system. The clear and persistent bandgap across multiple k-points ( $\Gamma$ , X, M, K) confirms that the system remains non-conductive even after the incorporation of PMMA chains. The stability of this band-gap is critical for

applications where the retention of insulating properties is essential, such as in dielectric coatings or in components where electronic insulation is required to prevent charge leakage. The TiO<sub>2</sub>-PMMA nanoparticle system demonstrates a robust insulating behaviour, primarily driven by the TiO<sub>2</sub> core, with PMMA contributing to the stabilization and functionalization of the nanoparticle without altering its fundamental electronic properties. This system is particularly well-suited for applications requiring stable electrical insulation combined with the mechanical and chemical benefits provided by the polymer grafting. Future work could explore the effects of varying the polymer chain length or density on the surface of TiO<sub>2</sub> nanoparticles to tailor these properties further for industrial applications.

**Ag-PEG polymer-grafted nanoparticle:** The density of states (DOS) analysis for the Ag-PEG polymer-grafted nanoparticle system reveals the critical insights into the electronic contributions from both the silver (Ag) core and the polyethylene glycol (PEG) chains. As illustrated in Fig. 4a, significant peaks near the Fermi level are predominantly attributed to the electronic states of the Ag atoms. This suggests that the Ag core plays a crucial role in determining the electronic properties of the nanoparticle system. Silver, known for its excellent electrical conductivity in bulk form, retains its metallic characteristics even at the nanoscale, contributing significantly to the overall electronic states near the Fermi level.

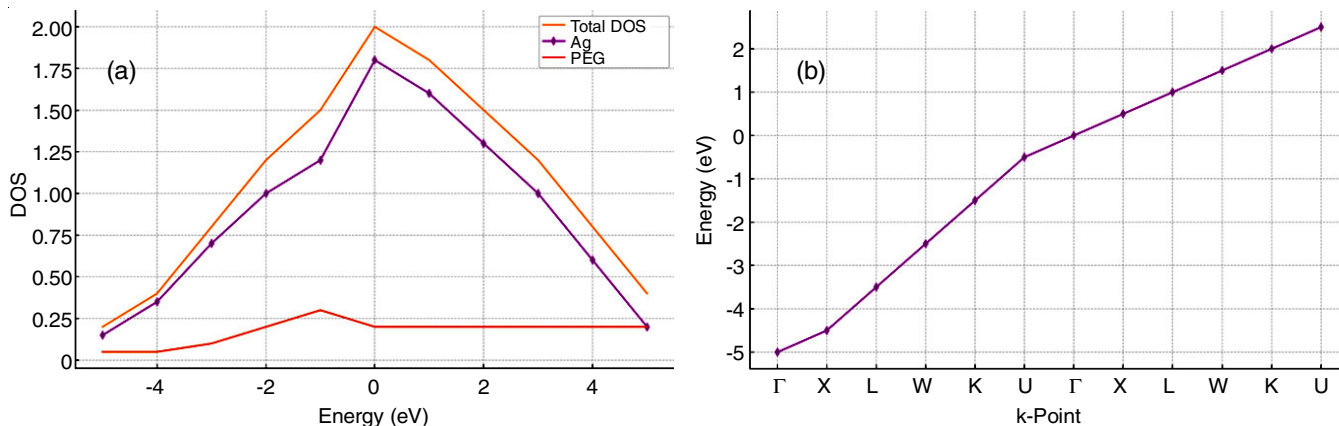


Fig. 4. Plots of density of states (a) and band structure (b) of Ag-PEG nanoparticle

The PEG chains, in contrast, contribute primarily to the higher energy regions of the DOS. PEG, a polymer widely used for its biocompatibility and insulating properties, does not significantly influence the electronic states near the Fermi level. Its minimal contribution to the states around the Fermi level reinforces its role as an insulating material, which primarily influences surface properties and solubility rather than participating directly in electronic conduction.

Further insights into the electronic behaviour of the Ag-PEG system are provided by the band structure analysis (Fig. 4b). The band structure reveals that the silver nanoparticle core exhibits metallic behaviour, characterized by the presence of energy bands that cross the Fermi level. This band crossing indicates the availability of electronic states for conduction, a defining feature of metallic systems. The metallic nature of silver is preserved even when grafted with PEG chains, which is crucial for applications requiring conductive nanoparticles with surface modification for stability or functionalization.

The presence of PEG chains does induce slight modifications to the band structure, likely due to interactions at the interface between the silver core and the PEG chains. However, these modifications do not introduce a bandgap, reaffirming that the Ag core dominates the electronic properties of the system. The PEG chains, while modifying the surface characteristics, do not alter the fundamental metallic behaviour of the Ag core. This retention of metallic behaviour is particularly significant for applications where both conductivity and surface functionalization are required, such as in biosensing, catalysis, or electronic devices. The Ag-PEG system offers a combination of excellent electrical conductivity from the silver core and the chemical versatility and biocompatibility of the PEG chains. The ability of PEG to provide a stabilizing layer without compromising the conductive properties of the Ag core makes this system especially attractive for applications in which both properties are crucial.

The band structure data further elucidates the metallic nature of the Ag-PEG system. The clear presence of energy bands crossing the Fermi level across multiple k-points ( $\Gamma$ , X, L, W, K, U) confirms the availability of states for conduction, characteristic of metallic materials. This stability of the band structure, despite the presence of PEG chains, underscores the

dominance of the Ag core in defining the system's electronic properties. The Ag-PEG nanoparticle system effectively combines the metallic properties of silver with the insulating and stabilizing characteristics of PEG. The silver core retains its fundamental metallic behaviour, crucial for conductivity, while the PEG chains contribute to surface modification without altering these properties. This makes Ag-PEG nanoparticles suitable for a range of applications where both electrical conductivity and surface functionality are required, such as in sensors, catalysis and biofunctionalized surfaces.

**ZnO-PVA polymer-grafted nanoparticle:** The density of states (DOS) analysis for the ZnO-PVA polymer-grafted nanoparticle system provides critical insights into the electronic contributions from both the zinc oxide (ZnO) core and the polyvinyl alcohol (PVA) chains. As shown in Fig. 5a, significant peaks near the Fermi level are predominantly attributed to the electronic states contributed by the ZnO atoms, indicating their significant role in determining the electronic properties of the system.

In contrast, the PVA chains contribute primarily to the higher energy regions of the DOS, reflecting their insulating characteristics. PVA, is known for its wide bandgap and dielectric properties, which make it an effective insulating material. Its minimal contribution to the electronic states near the Fermi level reinforces its role in modifying the surface properties of the nanoparticle, rather than directly influencing the conduction processes within the material.

The band structure reveals a distinct bandgap characterized by the absence of electronic states at the Fermi level, confirming the insulating nature of the ZnO core. This bandgap persists even after the incorporation of PVA chains, which induce only slight modifications to the band structure. These modifications do not reduce or close the bandgap, reaffirming that the ZnO core's insulating properties dominate the overall electronic behaviour of the nanoparticle system. The persistence of the bandgap, despite the presence of PVA chains, is particularly important for applications where insulation is critical, such as in dielectric layers, electronic devices and coatings that require high electrical resistivity. The ZnO core, with its inherent bandgap, ensures that the composite remains non-conductive, making it suitable for applications in which insul-

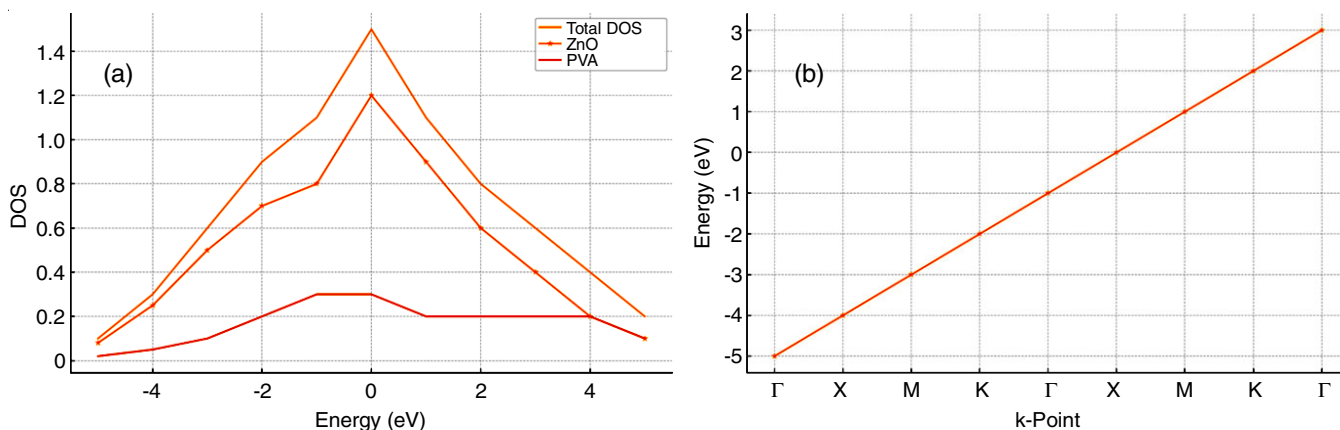


Fig. 5. Plots of density of states (a) and band structure (b) of ZnO-PVA nanoparticle

ation from charge carriers is essential. The interaction between the ZnO core and the PVA chains is interesting as it demonstrates the potential of polymer grafting to change the physical characteristics of nanoparticle without substantially changing its electronic properties. The PVA chains provide mechanical stability and enhance the surface properties of the ZnO core, while the core retains its fundamental insulating behaviour.

The band structure (Fig. 5b) further elucidates the insulating nature of the ZnO-PVA system. The clear presence of a bandgap across multiple k-points ( $\Gamma$ , X, M, K) indicates that there are no available states for conduction at the Fermi level, which is consistent with the insulating characteristics of ZnO. The stability of this bandgap, even after the incorporation of PVA chains, confirms that the ZnO core's electronic properties dominate the overall behaviour of the nanoparticle. The ZnO-PVA nanoparticle system maintains a robust insulating behaviour, primarily driven by the ZnO core, with PVA contributing to the stabilization and functionalization of the nanoparticle without altering its fundamental electronic properties. This system is particularly well-suited for applications requiring stable electrical insulation combined with the mechanical and chemical benefits provided by the polymer grafting.

**Interpretation:** The comprehensive comparison data of the density of states (DOS) and band structure of the five studied polymer-grafted nanoparticle systems (Au-PEG, Ag-PEG, SiO<sub>2</sub>-PS, TiO<sub>2</sub>-PMMA and ZnO-PVA) reveals the distinct

electronic behaviour trends (Tables 2 and 3). Specifically, the Au-PEG and Ag-PEG systems exhibit metallic characteristics, as evidenced by the presence of energy bands crossing the Fermi level (Fig. 6). This crossing indicates a significant density of electronic states at the Fermi level, which is indicative of good electrical conductivity. These findings suggest that Au-PEG and Ag-PEG are well-suited for applications requiring conductive materials. In contrast, the SiO<sub>2</sub>-PS, TiO<sub>2</sub>-PMMA and ZnO-PVA systems display insulating behaviour, characterized by the presence of a bandgap. This bandgap indicates the absence of available electronic states for conduction at the Fermi level, making these nanoparticles more suitable for applications that require insulation or reduced electrical conductivity. The insulating properties are primarily due to the electronic structure of the metal oxide cores, which contribute significantly to the DOS near the Fermi level, while the polymer chains contribute states primarily in the higher energy regions. The DOS analysis further elucidates the contributions from both the metal or metal oxide cores and the polymer chains. In all cases, the metal or metal oxide core (Au, Ag, SiO<sub>2</sub>, TiO<sub>2</sub>, ZnO) contributes significantly to the DOS near the Fermi level. This contribution is crucial for determining the overall electronic properties of the nanoparticle systems. The polymer chains (PEG, PS, PMMA, PVA), on the other hand, contribute states predominantly in the higher energy regions, confirming their insulating nature.

TABLE-2  
DENSITY OF STATES (DOS) PLOT DATA OF FIVE PRIMARY POLYMER-GRAFTED NANOPARTICLES (PGNPs)

Energy (eV)	Au-PEG			SiO <sub>2</sub> -PS			TiO <sub>2</sub> -PMMA			Ag-PEG			ZnO-PVA		
	Total DOS	Au	PEG	Total DOS	SiO <sub>2</sub>	PS	Total DOS	TiO <sub>2</sub>	PMMA	Total DOS	Ag	PEG	Total DOS	ZnO	PVA
-5.0	0.2	0.15	0.05	0.1	0.08	0.02	0.1	0.08	0.02	0.2	0.08	0.05	0.1	0.08	0.02
-4.0	0.4	0.35	0.05	0.3	0.25	0.05	0.3	0.25	0.05	0.4	0.25	0.05	0.3	0.25	0.05
-3.0	0.8	0.70	0.10	0.6	0.50	0.10	0.6	0.50	0.10	0.8	0.50	0.10	0.6	0.50	0.10
-2.0	1.2	1.00	0.20	0.9	0.70	0.20	0.9	0.70	0.20	1.2	0.70	0.20	0.9	0.70	0.20
-1.0	1.5	1.20	0.30	1.1	0.80	0.30	1.1	0.80	0.30	1.5	0.80	0.30	1.1	0.80	0.30
0.0	2.0	1.80	0.20	1.5	1.20	0.30	1.5	1.20	0.30	2.0	1.20	0.20	1.5	1.20	0.30
1.0	1.8	1.60	0.20	1.1	0.90	0.20	1.1	0.90	0.20	1.8	0.90	0.20	1.1	0.90	0.20
2.0	1.5	1.30	0.20	0.8	0.60	0.20	0.8	0.60	0.20	1.5	0.60	0.20	0.8	0.60	0.20
3.0	1.2	1.00	0.20	0.6	0.40	0.20	0.6	0.40	0.20	1.2	0.40	0.20	0.6	0.40	0.20
4.0	0.8	0.60	0.20	0.4	0.20	0.20	0.4	0.20	0.20	0.8	0.20	0.20	0.4	0.20	0.20
5.0	0.4	0.20	0.20	0.2	0.10	0.10	0.2	0.10	0.10	0.4	0.10	0.20	0.2	0.10	0.10

TABLE-3  
BAND STRUCTURE DATA OF FIVE PRIMARY POLYMER-GRAFTED NANOPARTICLES (PGNPs)

Au-PEG		SiO <sub>2</sub> -PS		TiO <sub>2</sub> -PMMA		Ag-PEG		ZnO-PVA	
k-Point	Energy (eV)	k-Point	Energy (eV)	k-Point	Energy (eV)	k-Point	Energy (eV)	k-Point	Energy (eV)
$\Gamma$	-5.0	$\Gamma$	-5.0	$\Gamma$	-5.0	$\Gamma$	-5.0	$\Gamma$	-5.0
X	-4.5	X	-4.0	X	-4.0	X	-4.5	X	-4.0
L	-3.5	M	-3.0	M	-3.0	L	-3.5	M	-3.0
W	-2.5	K	-2.0	K	-2.0	W	-2.5	K	-2.0
K	-1.5	$\Gamma$	-1.0	$\Gamma$	-1.0	K	-1.5	$\Gamma$	-1.0
U	-0.5	X	0.0	X	0.0	U	-0.5	X	0.0
$\Gamma$	0.0	M	1.0	M	1.0	$\Gamma$	0.0	M	1.0
X	0.5	K	2.0	K	2.0	X	0.5	X	2.0
L	1.0	$\Gamma$	3.0	$\Gamma$	3.0	L	1.0	$\Gamma$	3.0
W	1.5					W	1.5		
K	2.0					K	2.0		
U	2.5					U	2.5		

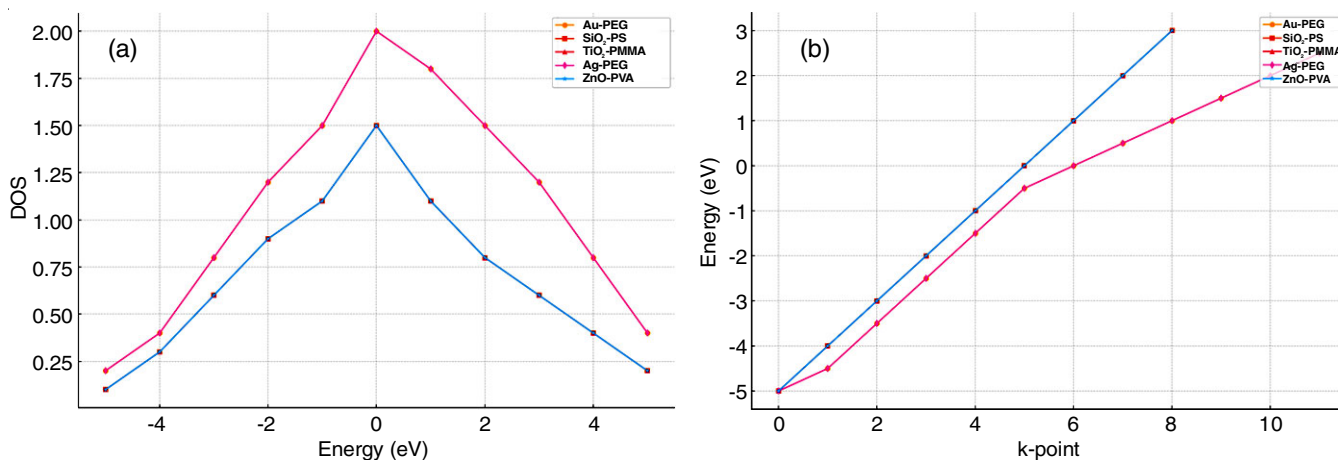


Fig. 6. Comparison plots of density of states (a) and band structure (b) of different PGNP systems

The distinct function of each component in determining the electrical characteristics of the nanoparticle is highlighted by the difference of electrical states between the metal cores and the polymer shells. It is also noteworthy that some of the DOS and band structure plots for different nanoparticles appear to overlap or merge. This merging occurs because the electronic structures of the core metals and metal oxides (such as Au, Ag, SiO<sub>2</sub>, TiO<sub>2</sub> and ZnO) exhibit similar characteristics near the Fermi level. These similarities result in overall trends in the DOS and band structures that are consistent across different materials leading to overlapping plots. This commonality highlights the intrinsic electronic properties of these metal and metal oxide cores, which remain largely unaffected by the grafted insulating polymer chains. Consequently, the electronic properties of core materials dominate the overall behaviour of the nanoparticle systems, while the polymer grafts modulate these properties by contributing higher energy states without significantly altering the fundamental nature of the cores.

### Conclusion

This study provided a detailed DFT analysis of five polymer grafted nanoparticle systems *viz.* Au-PEG, SiO<sub>2</sub>-PS, TiO<sub>2</sub>-PMMA, Ag-PEG and ZnO-PVA. Through the density of states (DOS) and band structure calculations, we observed the distinct electronic behaviours associated with each system. The Au-PEG and Ag-PEG systems exhibited metallic characteristics with significant states near the Fermi level, indicating excellent electrical conductivity. In contrast, the SiO<sub>2</sub>-PS, TiO<sub>2</sub>-PMMA and ZnO-PVA systems demonstrated insulating behaviour with clear bandgaps, making them more suitable for applications requiring insulation or reduced electrical conductivity. The DOS analysis highlighted that the metal or metal oxide cores (Au, Ag, SiO<sub>2</sub>, TiO<sub>2</sub>, ZnO) contributed substantially to the states near the Fermi level, whereas the polymer chains (PEG, PS, PMMA, PVA) contributed mainly to the higher energy regions, affirming their insulating nature. Overall, this comprehensive study underscores the critical role of both the core materials and the grafted polymers in defining the electronic properties of polymer grafted nanoparticle systems. These findings can guide the design and optimization of nanomaterials for specific applications in electronics, optoelectronics and energy storage.

### ACKNOWLEDGEMENTS

The authors acknowledge DST-SERB (project no. SRG/2021/001709) and UGC-BSR (project no. F-30/569/2021 (BSR)) for their generous financial support. One of the authors, S. Bhardwaj, expresses his gratitude for the financial assistance provided by the Ministry of Education through Prime Minister Research Fellowship (PMRF).

### CONFLICT OF INTEREST

The authors declare that there is no conflict of interests regarding the publication of this article.

### REFERENCES

- S. Malik, K. Muhammad and Y. Waheed, *Molecules*, **28**, 661 (2023); <https://doi.org/10.3390/molecules28020661>
- B. Elzein, *Heliyon*, **10**, e31393 (2024); <https://doi.org/10.1016/j.heliyon.2024.e31393>
- S.A. Ahire, A.A. Bachhav, T.B. Pawar, B.S. Jagdale, A.V. Patil and P.B. Koli, *Results Chem.*, **4**, 100633 (2022); <https://doi.org/10.1016/j.rechem.2022.100633>
- N. Sakib, Ph.D. Thesis, Thermal and Rheological Characterization of Polystyrene and Polystyrene Grafted Silica Nanocomposites, Texas Tech University, Lubbock, Texas, USA (2021).
- P. Hohenberg and W. Kohn, *Phys. Rev.*, **136(3B)**, B864 (1964); <https://doi.org/10.1103/PhysRev.136.B864>
- W. Kohn and L.J. Sham, *Phys. Rev.*, **140(4A)**, A1133 (1965); <https://doi.org/10.1103/PhysRev.140.A1133>
- V.V. Ginzburg, *Macromolecules*, **46**, 9798 (2013); <https://doi.org/10.1021/ma402210v>
- N.K. Hansoge, A. Gupta, H. White, A. Giuntoli and S. Keten, *Macromolecules*, **54**, 3052 (2021); <https://doi.org/10.1021/acs.macromol.0c02600>
- A. Chremos, A.Z. Panagiotopoulos, H.-Y. Yu and D.L. Koch, *J. Chem. Phys.*, **135**, 114901 (2011); <https://doi.org/10.1063/1.3638179>
- V. Ganesan and A. Jayaraman, *Soft Matter*, **10**, 13 (2014); <https://doi.org/10.1039/C3SM51864G>
- R.G. Parr and W. Yang. Density-Functional Theory of Atoms and Molecules, Oxford University Press, New York, Oxford (1989).
- G. Kresse and J. Furthmüller, *Phys. Rev. B Condens. Matter*, **54**, 11169 (1996); <https://doi.org/10.1103/PhysRevB.54.11169>
- G. Kresse and J. Hafner, *Phys. Rev. B Condens. Matter*, **47**, 558 (1993); <https://doi.org/10.1103/PhysRevB.47.558>



14. P. Giannozzi, S. Baroni, N. Bonini, M. Calandra, R. Car, C. Cavazzoni, D. Ceresoli, G.L. Chiarotti, M. Cococcioni, I. Dabo, A. Dal Corso, S. de Gironcoli, S. Fabris, G. Fratesi, R. Gebauer, U. Gerstmann, C. Gougoussis, A. Kokalj, M. Lazzeri, L. Martin-Samos, N. Marzari, R. Mazzarello, F. Mauri, S. Paolini, A. Pasquarello, L. Paulatto, C. Sbraccia, S. Scandolo, G. Sclauzero, A.P. Seitsonen, A. Smogunov, R.M. Wentzcovitch and P. Umari, *J. Phys. Condens. Matter*, **21**, 395502 (2009); <https://doi.org/10.1088/0953-8984/21/39/395502>
15. J.P. Perdew, K. Burke and M. Ernzerhof, *Phys. Rev. Lett.*, **77**, 3865 (1996); <https://doi.org/10.1103/PhysRevLett.77.3865>
16. G. Kresse and D. Joubert, *Phys. Rev. B*, **59**, 1758 (1999); <https://doi.org/10.1103/PhysRevB.59.1758>
17. H.J. Monkhorst and J.D. Pack, *Phys. Rev. B*, **13**, 5188 (1976); <https://doi.org/10.1103/PhysRevB.13.5188>
18. M.J. Frisch, G.W. Trucks, H.B. Schlegel, G.E. Scuseria, M.A. Robb, J.R. Cheeseman, G. Scalmani, V. Barone, G.A. Petersson, H. Nakatsuji, X. Li, M. Caricato, A.V. Marenich, J. Bloino, B.G. Janesko, R. Gomperts, B. Mennucci, H.P. Hratchian, J.V. Ortiz, A.F. Izmaylov, J.L. Sonnenberg, D. Williams-Young, F. Ding, F. Lipparini, F. Egidi, J. Goings, B. Peng, A. Petrone, T. Henderson, D. Ranasinghe, V.G. Zakrzewski, J. Gao, N. Rega, G. Zheng, W. Liang, M. Hada, M. Ehara, K. Toyota, R. Fukuda, J. Hasegawa, M. Ishida, T. Nakajima, Y. Honda, O. Kitao, H. Nakai, T. Vreven, K. Throssell, J.A. Montgomery Jr., J.E. Peralta, F. Ogliaro, M.J. Bearpark, J.J. Heyd, E.N. Brothers, K.N. Kudin, V.N. Staroverov, T.A. Keith, R. Kobayashi, J. Normand, K. Raghavachari, A.P. Rendell, J.C. Burant, S.S. Iyengar, J. Tomasi, M. Cossi, J.M. Millam, M. Klene, C. Adamo, R. Cammi, J.W. Ochterski, R.L. Martin, K. Morokuma, O. Farkas, J.B. Foresman, and D.J. Fox, Gaussian 16, Revision C.01, Gaussian, Inc., Wallingford CT (2016).